Environmental Research Letters

LETTER

Simulation of air and ground temperatures in PMIP3/CMIP5 last millennium simulations: implications for climate reconstructions from borehole temperature profiles

A García-García[1], F J Cuesta-Valero[1], H Beltrami[1,2,4] and J E Smerdon[3]

[1] Climate & Atmospheric Sciences Institute and Department of Earth Sciences, St. Francis Xavier University, Antigonish, Nova Scotia, Canada
[2] Centre ESCER pour l'étude et la simulation du climate à l'échelle régionale, Université du Québec à Montréal, Canada
[3] Lamont-Doherty Earth Observatory, Columbia University, Palisades, New York, USA
[4] Author to whom any correspondence should be addressed.

E-mail: hugo@stfx.ca

Keywords: air–ground coupling, millennium simulations, borehole temperature profiles

OPEN ACCESS

RECEIVED
15 November 2015

REVISED
29 February 2016

ACCEPTED FOR PUBLICATION
10 March 2016

PUBLISHED
20 April 2016

Abstract

For climate models to simulate the continental energy storage of the Earth's energy budget they must capture the processes that partition energy across the land-atmosphere boundary. We evaluate herein the thermal consequences of these processes as simulated by models in the third phase of the paleoclimate modelling intercomparison project and the fifth phase of the coupled model intercomparison project (PMIP3/CMIP5). We examine air and ground temperature tracking at decadal and centennial time-scales within PMIP3 last-millennium simulations concatenated to historical simulations from the CMIP5 archive. We find a strong coupling between air and ground temperatures during the summer from 850 to 2005 CE. During the winter, the insulating effect of snow and latent heat exchanges produce a decoupling between the two temperatures in the northern high latitudes. Additionally, we use the simulated ground surface temperatures as an upper boundary condition to drive a one-dimensional conductive model in order to derive synthetic temperature-depth profiles for each PMIP3/CMIP5 simulation. Inversion of these subsurface profiles yields temperature trends that retain the low-frequency variations in surface air temperatures over the last millennium for all the PMIP3/CMIP5 simulations regardless of the presence of seasonal decoupling in the simulations. These results demonstrate the robustness of surface temperature reconstructions from terrestrial borehole data and their interpretation as indicators of past surface air temperature trends and continental energy storage.

1. Introduction

Recent increases in global surface temperatures (Field *et al* 2014) are the result of the Earth's energy imbalance arising mainly from an increase in the atmospheric concentration of greenhouse gases (Hansen *et al* 2011, von Schuckmann *et al* 2016). These changes affect all of Earth's climate subsystems: atmosphere, ocean, land and cryosphere (Levitus *et al* 2001, Beltrami *et al* 2002, Huang 2006, Hansen *et al* 2010, Lyman *et al* 2010, Zwally *et al* 2011). Although most of the Earth's recent energy gains have been stored in the ocean, the land surface has stored the second largest amount and is a critical factor in the evolution of processes such as permafrost melting, which is potentially an important positive feedback within the climate system (Knorr *et al* 2005, Lawrence *et al* 2008). Correctly simulating the energy storage in each climate subsystem, including the continental component of the Earth's energy budget, is therefore important for general circulation models (GCMs) to produce robust future climate change projections under different emission scenarios, and to assess the future evolution of potentially important climate feedback processes in the shallow subsurface (Hansen *et al* 2005, Koven *et al* 2013).

Estimates of heat gain in the continental subsurface prior to widespread instrumental observations are those obtained from geothermal data by direct interpretation of the data at the local scale. At global scales, the subsurface heat gain is indirectly inferred from ground surface temperature (GST) histories from borehole temperature profiles. Interpretations of GST histories from geothermal data as indicators of climate change nevertheless assume a long-term thermal coupling between the lower atmosphere and the continental subsurface (Beltrami 2002, Beltrami *et al* 2002). Multiple studies have shown evidence that supports this assumption at decades and longer time scales (González-Rouco *et al* 2003, Chapman *et al* 2004, Pollack and Smerdon 2004). In contrast, some studies have pointed to the decoupling between high-latitude air and ground temperatures in winter, because of long-term changes in snow cover (Mann *et al* 2003, Mann and Schmidt 2003, Stieglitz *et al* 2003). Such impacts could induce a potential bias in surface-temperature reconstructions from geothermal data (Pollack and Huang 2000, González-Rouco *et al* 2006), but the extent and impact of decoupling on decadal and longer timescales is a matter of debate (González-Rouco *et al* 2003, 2006, Chapman *et al* 2004, Pollack and Smerdon 2004).

In this paper, we use the set of last-millennium (LM) model experiments from the third phase of the paleoclimate modelling intercomparison project (PMIP3) and the fifth phase of the coupled model intercomparison project (CMIP5), to test a fundamental assumption of borehole paleoclimatology: near-surface air and ground temperature changes are strongly coupled over decades to centuries, making inversions of terrestrial borehole temperature profiles representative of surface air temperature changes over such timescales. This assumption is tested across the ensemble of PMIP3/CMIP5 GCM LM simulations, which, in contrast to earlier experiments that used a single model, includes a larger set of state-of-the-art GCMs with different configurations and initial conditions, as well as a variety of land-surface model components responsible for simulating the energy partitioning at the air–ground interface. These simulations additionally include a larger representation of last millennium forcings (Schmidt *et al* 2011, 2012) than used in the GKSS ECHO-g LM simulations (Crowley 2000, González-Rouco *et al* 2003, 2006). The PMIP3/CMIP5 ensemble therefore includes a broader representation of the effect of different climate forcings on long-term air–ground coupling. For instance, the CMIP5 simulations include the effect of aerosol forcing, a factor that was not taken into account in the ECHO-g past millennium simulations. Our analysis therefore is the first to use a state-of-the-art ensemble of LM climate model simulations to evaluate the effects of the seasonal relationships between air and ground temperatures and the ability of temperature-profile inversion schemes to recover changes in surface air temperatures over decades and centuries.

2. Data and methods

We use LM PMIP3 simulations (Braconnot *et al* 2012) and historical CMIP5 (Taylor *et al* 2012) simulations from the models listed in table 1. The PMIP3 simulations are performed with the same configurations and resolutions as the corresponding GCMs in the CMIP5 experiments, allowing direct evaluation of the paleoclimate simulations in conjunction with the historical runs. We do not use two GCM simulations in the PMIP3/CMIP5 archive: the MIROC-ESM model has a long-term temperature drift (Sueyoshi *et al* 2013) and the complete ground temperature output for the IPSL-CM5A-LR LM simulation was not available on the Earth System Grid Federation's server.

The temporal interval of our analysis is defined by the LM simulations that extend from 850 to 1850 common era (CE), concatenated to the CMIP5 Historical simulations (Mieville *et al* 2010), spanning the period from 1850 to 2005 CE. Although LM and historical simulations are not a single continuous simulation, the discontinuity for the variables employed at 1850 CE falls within the range of the simulated climate variability (e.g. Coats *et al* 2014). We use the monthly surface air temperature at 2 m (SAT, tas in the CMIP5 variable catalogue), as well as the monthly GST, linearly interpolated to a depth of 1 m (GST, tsl in the CMIP5 variable catalogue) in order to have a reference depth for all models (e.g. Koven *et al* 2013). We also use the deepest subsurface temperature layer (DST) of each model.

In order to verify the methodology for reconstructing GST histories from borehole temperature profiles, we also employ a purely conductive 1D forward model (Beltrami and Mareschal 1992, Beltrami *et al* 1992), which uses the anomalies of the PMIP3/CMIP5 simulated air and ground temperatures as upper boundary conditions on a semi-infinite homogeneous half space, with a zero-flux bottom boundary condition. This forward model is used to generate synthetic profiles to a depth of 500 m. Subsequently, the synthetic profiles are inverted to retrieve the surface-temperature histories, following the singular value decomposition method of inversion to reconstruct surface-temperature histories from geothermal data (Mareschal and Beltrami 1992).

3. Results

The mean annual global SAT, continental SAT, GST and DST anomalies, from 850 to 2005 CE with respect to their 1900–1990 CE means are highly correlated at multi-decadal time scales (figure 1 and table 2). Global and continental SAT anomalies (figure 1) display some differences in their respective global means for the five

Table 1. General circulation models (GCMs) used in this analysis, the land-surface component of the GCMs, the total simulated subsurface depth, the depth of the deepest subsurface temperature (DST), the number of subsurface layers and the land-surface component references.

Model name	Land model	Subsurface depth (m)	DST layer depth (m)	Number of subsurface layers	Land model reference
BCC-CSM1.1	BCC-AVIM1.0	3.43	2.86	10	Wu *et al* (2013)
CCSM4.0	CLM4	43.74	35.18	15	Oleson *et al* (2010)
GISS-E2-R	GISS-LSM	3.5	2.73	6	Rosenzweig and Abramopoulos (1997)
MPI-ESM-P	JSBATH	9.58	6.98	5	Roeckner *et al* (2003)
MRI-CGCM3	HAL	10	8.5	14	Yukimoto *et al* (2012)

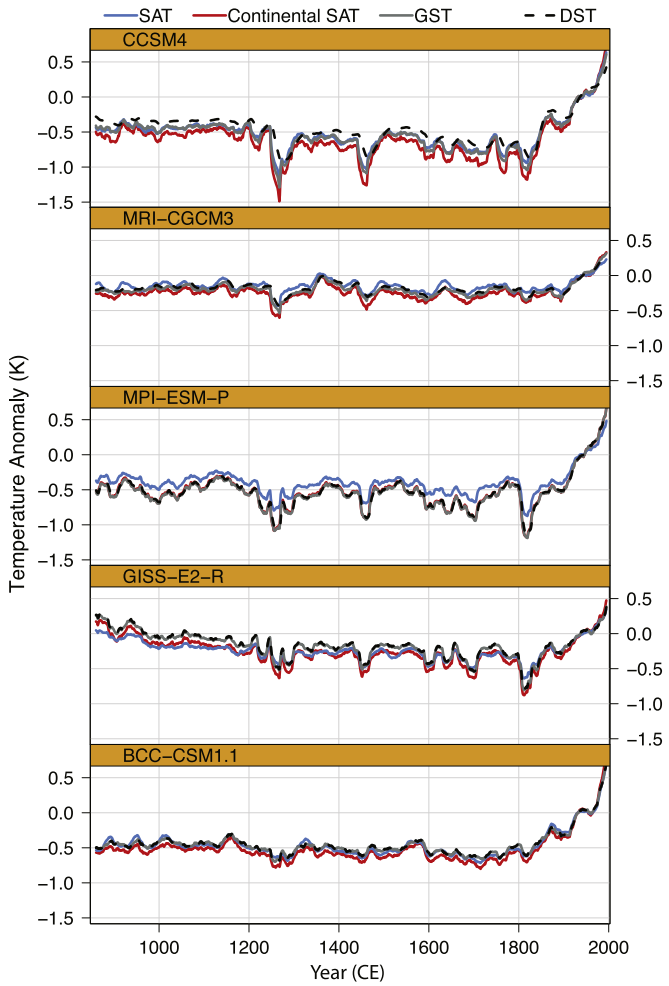

Figure 1. The 21-year running mean of simulated temperature anomalies relative to 1900–1990 CE, using global annual surface air temperature (SAT), annual SAT over the continental areas, annual ground surface temperature at 1 m (GST) and annual subsurface temperature at the deepest layer (DST) from each PMIP3/CMIP5 simulation (sorted in descending order of the deepest soil layer in each model).

Table 2. Temporal correlation coefficients between global temperatures from 850 to 2005 CE (from 850 to 1900 CE in brackets) for the annual and the 21-year filtered time series. Employed variables are the surface air temperature (SAT), annual SAT over the continental areas (Continental SAT), annual ground surface temperature at 1 m (GST) and annual subsurface temperature at the deepest layer (DST) from each PMIP3/CMIP5 simulation. All of the correlation coefficients are significant at the 95% level using a phase-randomizing bootstrapping technique with 1000 Monte Carlo runs (Ebisuzaki 1997).

Annual temp. correlation	CCSM4	MRI-CGCM3	MPI-ESM-P	GISS-E2-R	BCC-CSM1.1
SAT versus Continental SAT	0.97 (0.96)	0.93 (0.90)	0.97 (0.96)	0.95 (0.95)	0.96 (0.90)
SAT versus DST	0.75 (0.54)	0.62 (0.44)	0.86 (0.76)	0.91 (0.93)	0.94 (0.83)
SAT versus GST	0.97 (0.96)	0.88 (0.84)	0.97 (0.96)	0.93 (0.94)	0.95 (0.85)
Continental SAT versus DST	0.67 (0.45)	0.58 (0.35)	0.85 (0.75)	0.95 (0.95)	0.94 (0.85)
Continental SAT versus GST	0.97 (0.96)	0.89 (0.84)	0.99 (0.98)	0.97 (0.97)	0.95 (0.87)
DST versus GST	0.74 (0.59)	0.74 (0.59)	0.90 (0.83)	0.99 (0.99)	0.99 (0.99)
21-y filtered temp. correlation	**CCSM4**	**MRI-CGCM3**	**MPI-ESM-P**	**GISS-E2-R**	**BCC-CSM1.1**
SAT versus Continental SAT	0.99 (0.98)	0.96 (0.94)	0.99 (0.98)	0.97 (0.97)	0.98 (0.95)
SAT versus DST	0.93 (0.88)	0.89 (0.80)	0.98 (0.97)	0.93 (0.97)	0.98 (0.95)
SAT versus GST	0.99 (0.99)	0.93 (0.89)	0.99 (0.98)	0.94 (0.97)	0.98 (0.95)
Continental SAT versus DST	0.92 (0.85)	0.92 (0.85)	0.99 (0.98)	0.98 (0.99)	0.99 (0.98)
Continental SAT versus GST	0.99 (0.99)	0.97 (0.95)	0.99 (0.99)	0.98 (0.99)	0.99 (0.98)
DST versus GST	0.94 (0.89)	0.97 (0.95)	0.99 (0.99)	0.99 (0.99)	0.99 (0.99)

Table 3. Seasonal temporal correlation coefficients between temperatures in NH extratropical areas (27° N −90°N, 180° W −180°E), from 850 to 2005 CE (from 850 to 1900 CE in brackets) for the annual and the 21-year filtered time series. Employed variables are the SAT over the continental areas (Continental SAT), ground surface temperature at 1 m (GST) and annual subsurface temperature at the deepest layer (DST) from each PMIP3/CMIP5 simulation. All of the correlation coefficients are significant 95% level using a phase-randomizing bootstrapping technique with 1000 Monte Carlo runs (Ebisuzaki 1997).

Annual temp. correlation	CCSM4	MRI-CGCM3	MPI-ESM-P	GISS-E2-R	BCC-CSM1.1
NH Winter Continental SAT versus DST	0.53 (0.34)	0.34 (0.16)	0.70 (0.59)	0.72 (0.69)	0.63 (0.39)
NH Summer Continental SAT versus DST	0.53 (0.34)	0.44 (0.23)	0.66 (0.54)	0.88 (0.88)	0.81 (0.66)
NH Winter Continental SAT versus GST	0.77 (0.69)	0.55 (0.47)	0.92 (0.91)	0.78 (0.75)	0.64 (0.42)
NH Summer Continental SAT versus GST	0.93 (0.92)	0.80 (0.74)	0.96 (0.96)	0.94 (0.94)	0.92(0.86)
NH Winter DST versus GST	0.75 (0.59)	0.71 (0.58)	0.84 (0.76)	0.98 (0.98)	0.95 (0.92)
NH Summer DST versus GST	0.69 (0.50)	0.61 (0.38)	0.81 (0.69)	0.98 (0.98)	0.96 (0.92)
21-y filtered temp. correlation	**CCSM4**	**MRI-CGCM3**	**MPI-ESM-P**	**GISS-E2-R**	**BCC-CSM1.1**
NH Winter Continental SAT versus DST	0.88 (0.79)	0.79 (0.63)	0.96 (0.93)	0.91 (0.93)	0.94 (0.83)
NH Summer Continental SAT versus DST	0.89 (0.82)	0.88 (0.77)	0.96 (0.93)	0.97 (0.97)	0.95 (0.82)
NH Winter Continental SAT versus GST	0.96 (0.93)	0.83 (0.74)	0.98 (0.97)	0.94 (0.94)	0.94 (0.82)
NH Summer Continental SAT versus GST	0.98 (0.97)	0.94 (0.86)	0.98 (0.97)	0.98 (0.98)	0.97 (0.92)
NH Winter DST versus GST	0.94 (0.90)	0.96 (0.93)	0.98 (0.97)	0.99 (0.99)	0.99 (0.97)
NH Summer DST versus GST	0.92 (0.87)	0.91 (0.83)	0.98 (0.96)	0.99 (0.99)	0.99 (0.96)

simulations. The evolution of these anomalies, however, is highly correlated (>0.9) at decadal to century times scales. If the last century is not taken into account, the correlation values are smaller, but still highly significant (see tables 2 and 3). As expected, the global SAT anomalies are warmer than the continental SAT anomalies for most of the simulation period in all models, due to the well-known differences between ground and ocean thermal properties. Over the continental areas, global GST and DST are warmer than SAT for all the PMIP3/CMIP5 simulations, except for the MPI-ESM-P, in which the continental SAT, GST and DST anomalies are similar throughout the simulation. In the subsurface, the global GST and DST anomalies are identical for the shallow GCMs, showing correlations $\geqslant$0.9 in the BCC-CSM1.1, GISS-E2-R and MPI-ESM-P models, while correlations are slightly reduced (~0.7) for the CCSM4 (bottom boundary at 43.74 m) and MRI-CGCM3 (bottom boundary at 10 m) simulations. These differences between shallow and deep model temperature anomalies are due to the larger attenuation and phase-shift of the subsurface temperatures at the deepest layer for the deep GCMs in relation to the shallow bottom boundary GCMs (Smerdon and Stieglitz 2006).

These results suggest the existence of a strong coupling between GST and SAT over continental areas at time-scales from decades to centuries, although some studies have noted seasonal differences in the air–ground thermal relationship (González-Rouco *et al* 2003, Lin *et al* 2003, Mann and Schmidt 2003, Stieglitz *et al* 2003, Chapman *et al* 2004, Schmidt and Mann 2004, Smerdon *et al* 2006). To study the seasonal effect of winter and summer on the air and ground temperature relationships within the PMIP3/CMIP5 past millennium simulations, we evaluated the continental SAT, GST and DST anomalies in the north hemisphere (NH) extratropical areas (27 ° N–90° N, 180° W–180° E) in winter (December, January and February) and summer (June, July and August) separately (figure 2). In NH summer, the continental SAT, GST and DST anomalies are similar for all of the simulations, showing a stable temporal coupling and high correlation between air and subsurface temperatures (figure 2, right panel; table 3). Air and subsurface temperature anomalies in NH winter (figure 2, left panel) show some decoupling, with GST and DST warmer than continental SAT for four of the simulations. The one exception is the MPI-ESM-P simulation, in which the coupling remains nearly constant in both seasons. Winter decoupling across the ensemble of models is reflected in the correlation coefficients; all the models show lower correlation coefficients between continental SAT and GST in NH winter than in NH summer, except the MPI-ESM-P model that shows correlations of 0.9 independent of the season.

To explore the possible causes of winter decoupling within the PMIP3/CMIP5 simulations we compute the correlation coefficients in each grid-point between SAT and GST from 850 to 2005 CE seasonly for the globe. The correlation in NH summer (June, July and August, annual mean) between SAT and GST (figure 3, right panels) shows high correlation coefficients globally, except in areas where freezing phenomena persists during the summer. This behaviour appears in four of the GCMs, but the MPI-ESM-P simulation yields correlation coefficients that are high globally. In the NH winter (December, January and February, annual mean) (figure 3, left panels), the correlation coefficients between SAT and GST decrease for the five simulations in the northern hemisphere. High correlation coefficients remain in the southern hemisphere. For the BCC-CSM1.1, GISS-E2-R, MRI-CGCM3 and CCSM4 simulations, the correlation coefficients decrease to less than 0.5 in part of North America and Eurasia, where the presence of snow and

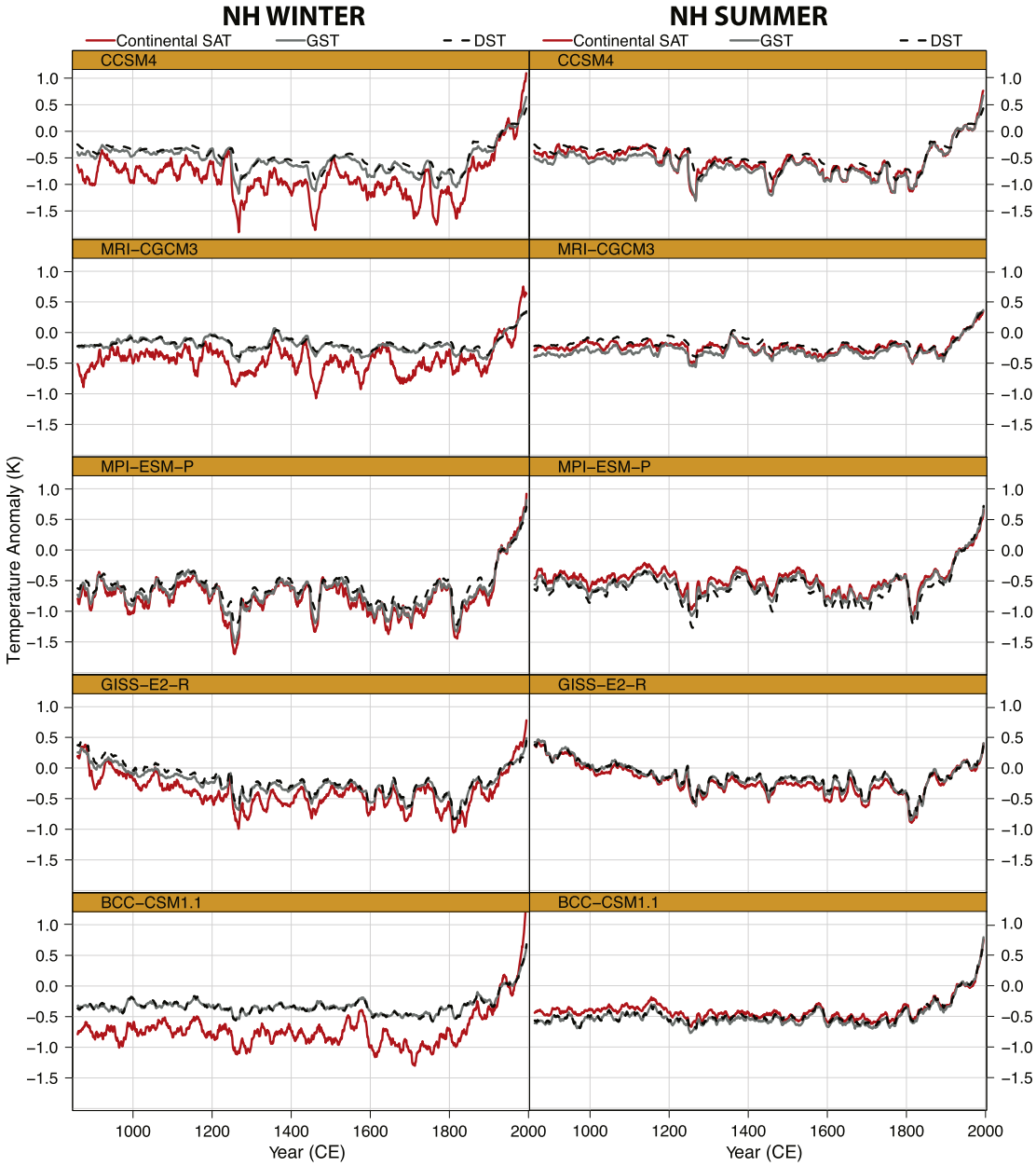

Figure 2. The 21-year running mean of simulated anomalies relative to 1900–1990 CE in NH extratropical areas (27° N–90° N, 180° W–180° E), using continental SAT, GST and DST in NH winter (December, January and February annual mean, left column) and NH summer (June, July and August annual mean, right column).

freezing phenomena are expected to cause decoupling on annual timescales (e.g. Kane *et al* 2001, Sokratov and Barry 2002, Beltrami and Kellman 2003, Smerdon *et al* 2003, 2004, Stieglitz *et al* 2003, Smerdon and Stieglitz 2006). Although the correlation coefficients in NH winter decrease with respect to those in NH summer in the MPI-ESM-P simulation, this decrease is weak and the correlation coefficients remain high globally in both seasons. The decrease of the correlation coefficients in snow covered areas for the PMIP3/CMIP5 simulations reinforces the importance of the insulating effect of snow cover on air–ground coupling. The strong air–ground coupling in NH winter and NH summer for the MPI-ESM-P simulation may be due to the use of the same value of the thermal conductivity for frozen and thawed subsurface, as well as other snow properties defined in the land-surface component of the model (JSBACH) (Koven *et al* 2013, table 1). The correlation coefficients between SAT and GST are also higher when the time series are filtered with a 21-year running mean to focus on low-frequency behaviour, which was also shown in (González-Rouco *et al* 2003, 2006) (figure 4). The 21-year filtered spatial correlation patterns remain similar to the annual correlation patterns, although the correlation coefficients are universally larger for the filtered quantities. This behaviour is present for the five model simulations, indicating that at low frequencies the coupling between air and ground temperatures is enhanced.

The correlation coefficients also display spatial variability over areas where snow cover is not present

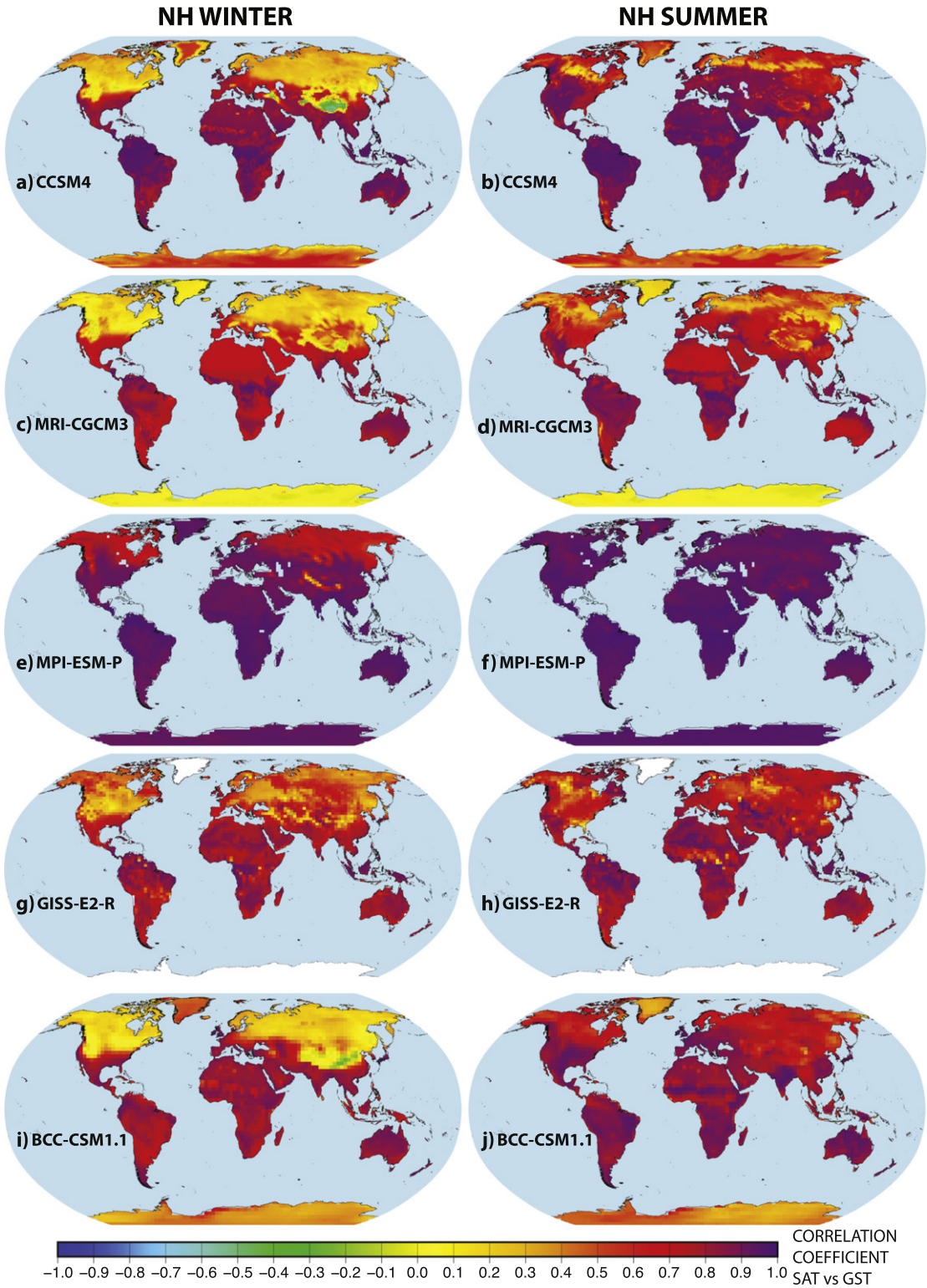

Figure 3. Seasonal correlation coefficients between SAT and GST in continental areas over the period 850–2005 CE. December, January and February annual mean on (a) (CCSM4), (c) (MRI-CGCM3), (e) (MPI-ESM-P), (g) (GISS-E2-R) and (i) (BCC-CSM1.1) panels. June, July and August annual mean on (b) (CCSM4), (d) (MRI-CGCM3), (f) (MPI-ESM-P), (h) (GISS-E2-R) and (j) (BCC-CSM1.1) panels.

(figures 3 and 4), likely due to factors such as the spatial variation of moisture (Dirmeyer 2011) and vegetation cover, the latter of which increases latent heat fluxes through evapotranspiration (Bonan 2001). Local correlation coefficients between SAT and GST are enhanced through the tropics in the MRI and GISS models, but areas of low vegetation such as the Sahara desert also have large correlation coefficients in multiple models during both the NH summer and winter. Multiple non-cryogenic processes are therefore relevant to the coupling between SAT and GST temperatures that are simulated

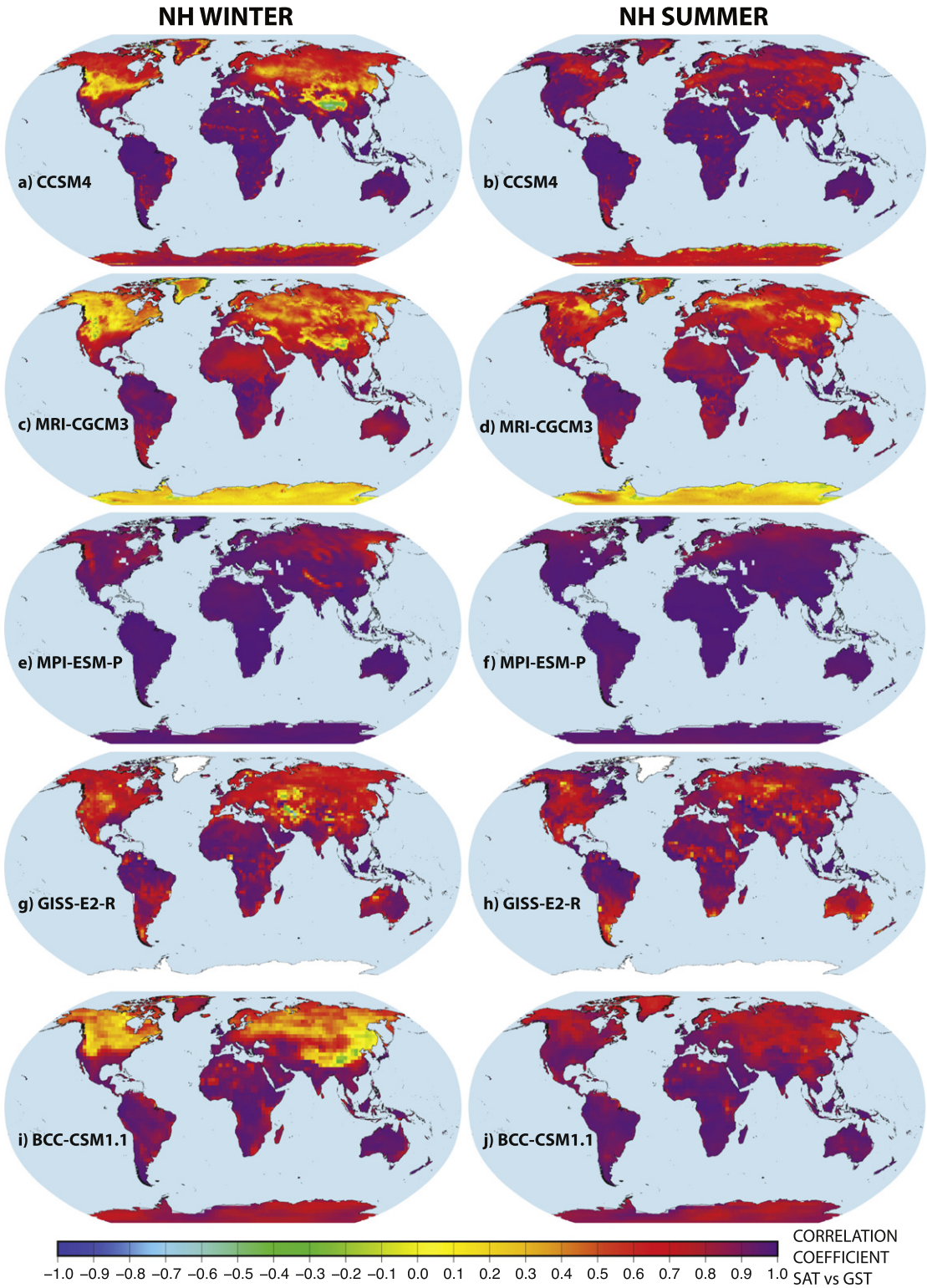

Figure 4. Seasonal correlation coefficients between 21-year filtered SAT and GST in continental areas over the period 850–2005 CE. December, January and February annual mean on (a) (CCSM4), (c) (MRI-CGCM3), (e) (MPI-ESM-P), (g) (GISS-E2-R) and (i) (BCC-CSM1.1) panels. June, July and August annual mean on (b) (CCSM4), (d) (MRI-CGCM3), (f) (MPI-ESM-P), (h) (GISS-E2-R) and (j) (BCC-CSM1.1) panels.

differently across the model ensemble. It is beyond the scope of this investigation to diagnose each of those processes and their impact on the coupling between air and ground temperatures, rather it is sufficient to note that they impact the coupling by differing degrees within each of the models and have different temporal signatures based on the annual and 21-year filtered correlation patterns.

Regardless of the underlying seasonal processes that cause short-term coupling variations, we can asses the possibility that they may alter the surface-temperature histories reconstructed from geothermal

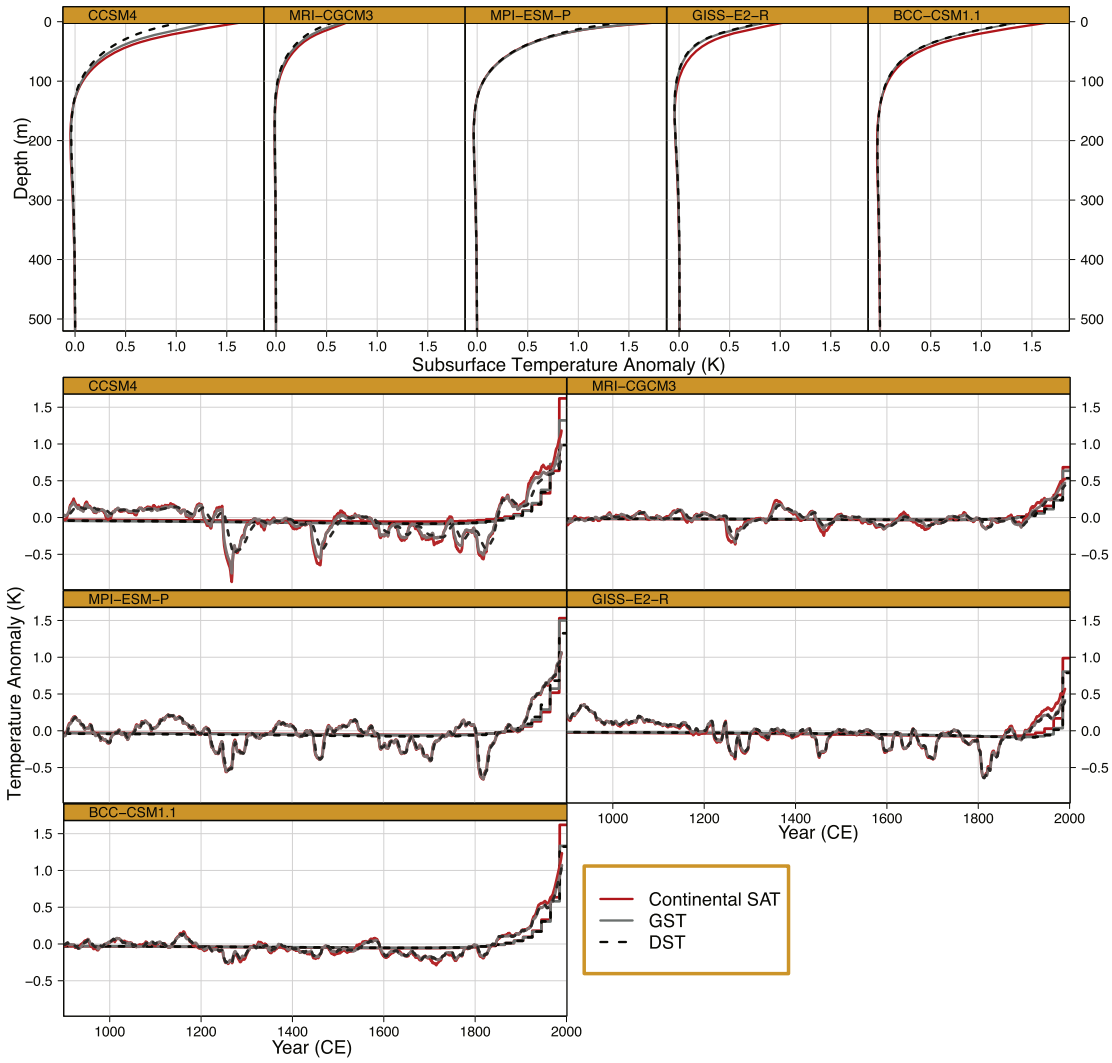

Figure 5. (Top) Synthetic subsurface temperature anomaly profiles driven as upper boundary conditions by global annual continental SAT, GST and DST anomalies relative to 850–2005 CE over all the continental grid cells of each model. (bottom) The 21-year running mean of the global temperature anomalies relative to 850–2005 CE, using SAT, GST and DST from the PMIP3/CMIP5 simulations and the synthetic surface-temperature histories derived from the inversion of the synthetic subsurface temperature profiles, shown as series of step changes in temperature.

data, by generating synthetic subsurface temperature anomaly profiles from the PMIP3/CMIP5 continental SAT, GST and DST anomalies. We do so using an idealized semi-infinite homogenous subsurface model as described in the data and methods section to generate profiles at all locations on the continents. Although the network of borehole measurements samples a subset of global land grids, González-Rouco *et al* (2006) demonstrated that the network sampling was sufficient for estimating results from a complete representation of the global land grid. We therefore use a complete sampling of continental grid points as representative of results from a subsampling of grid cells based on the actual distribution of the borehole network. The synthetic temperature anomaly profiles are then inverted to obtain the corresponding ground surface-temperature histories, following standard borehole climatology methods for reconstructing the past millennium temperature changes (e.g. Mareschal and Beltrami 1992). The synthetic subsurface temperature profiles (figure 5) derived from the SAT, GST and the DST anomalies as upper boundary conditions, show similar profiles across the five simulations. In all cases, each profile shows a different subsurface temperature anomaly in the upper 100 m, as a response to each time history of the simulated SAT anomalies. Most importantly, however, the GST histories recovered by inversion of each subsurface temperature anomaly profile retain the low-frequency changes in the air and subsurface temperatures of each model simulation. These results support the ability of borehole climatology methods to reconstruct surface-temperature histories from geothermal data, in spite of seasonal decoupling processes. With regard to snow cover specifically, the absence of a low-frequency influence is likely due to the fact that simulated changes in the snow cover

thickness and length of snow cover season do not change significantly over the simulation period (Goodrich 1982).

4. Conclusions

Results support the assumption that air–ground thermal coupling is strong on global and regional spatial scales and over decades and centuries within the PMIP3/CMIP5 last millennium simulations. In NH winter particularly, the PMIP3/CMIP5 simulations show a short-term decoupling in the northern high latitudes, due to the insulating effect of snow cover. Because these seasonal variations of temperature do not penetrate more than a few metres into the subsurface, however, the short-term decoupling does not affect the GST histories retrieved from geothermal data. Furthermore, inversions recover the GST histories from the temperature trends of the PMIP3/CMIP5 temperature simulations.

The above conclusions are consistent with those of (González-Rouco *et al* 2003, 2006) despite significant differences between the earlier GKSS ECHO-g model and the state-of-the-art GCMs from the PMIP3/CMIP5 ensemble used herein. In particular, these conclusions stand across a collection of models with different land-surface model components. The earlier ECHO-g simulations also use different external forcings and did not include aerosol forcings. Despite each of these differences and the diversity of models across the PMIP3/CMIP5 ensemble, the thermal coupling between the lower atmosphere and the continental subsurface is maintained over decades to centuries within the five PMIP3/CMIP5 GCM simulations, validating the interpretation of underground temperatures as indicators of climatic change on decades to centuries. These findings also add to the now large body of work supporting the use of borehole reconstructions in the ensemble of proxy-estimated temperatures of the last millennium and the importance of the borehole estimates as benchmarks for low-frequency temperature change over the last 500–1000 years.

Acknowledgments

We are grateful for two constructive reviews that helped us to improve this communication. This work was supported by grants from the Natural Sciences and Engineering Research Council of Canada Discovery Grant (NSERC DG 140576948), a NSERC-CREATE award *Training Program in Climate Sciences* and the Atlantic Computational Excellence Network (ACEnet), the Atlantic Innovation Fund (AIF-ACOA) to H Beltrami. H Beltrami holds Canada Research Chair. A G G and F J C V are funded by a NSERC-CREATE *Training Program in Climate Sciences* based at St.Francis Xavier University. Lamont-Doherty Earth Observatory contribution number 7993.

References

Beltrami H 2002 Climate from borehole data: energy fluxes and temperatures since 1500 *Geophys. Res. Lett.* **29** 26-1–26-4

Beltrami H, Jessop A M and Mareschal J-C 1992 Ground temperature histories in eastern and central Canada from geothermal measurements: evidence of climatic change *Glob. Planet. Change* **6** 167–83

Beltrami H and Kellman L 2003 An examination of short- and long-term air–ground temperature coupling *Glob. Planet. Change* **38** 291–303

Beltrami H and Mareschal J-C 1992 Ground temperature histories for central and eastern Canada from geothermal measurements: little ice age signature *Geophys. Res. Lett.* **19** 689–92

Beltrami H, Smerdon J E, Pollack H N and Huang S 2002 Continental heat gain in the global climate system *Geophys. Res. Lett.* **29** 8-1–8-3

Bonan G B 2001 Observational evidence for reduction of daily maximum temperature by croplands in the midwest United States *J. Clim.* **14** 2430–42

Braconnot P, Harrison S P, Kageyama M, Bartlein P J, Masson-Delmotte V, Abe-Ouchi A, Otto-Bliesner B and Zhao Y 2012 Evaluation of climate models using palaeoclimatic data *Nat. Clim. Change* **2** 417–24

Chapman D S, Bartlett M G and Harris R N 2004 Comment on ground versus surface air temperature trends: implications for borehole surface temperature reconstructions by M E Mann and G Schmidt *Geophys. Res. Lett.* **31** L07205

Coats S, Smerdon J E, Cook B I and Seager R 2014 Are simulated megadroughts in the north american southwest forced? *J. Clim.* **28** 124–42

Crowley T J 2000 Causes of climate change over the past 1000 years *Science* **289** 270–7

Dirmeyer P A 2011 The terrestrial segment of soil moisture-climate coupling *Geophys. Res. Lett.* **38** L16702

Ebisuzaki W 1997 A method to estimate the statistical significance of a correlation when the data are serially correlated *J. Clim.* **10** 2147–53

Field C B *et al* 2014 Technical summary *Climate Change 2014: Impacts, Adaptation, and Vulnerability. Part A: Global and Sectoral Aspects. Contribution of Working Group II to the Fifth Assessment Report of the Intergovernmental Panel on Climate Change* ed C B Field *et al* (Cambridge: Cambridge University Press) pp 35–94

González-Rouco F, von Storch H and Zorita E 2003 Deep soil temperature as proxy for surface air-temperature in a coupled model simulation of the last thousand years *Geophys. Res. Lett.*. **30** 2116

González-Rouco J F, Beltrami H, Zorita E and von Storch H 2006 Simulation and inversion of borehole temperature profiles in surrogate climates: spatial distribution and surface coupling *Geophys. Res. Lett.* **33** L01703

Goodrich L 1982 The influence of snow cover on the ground thermal regime *Can. Geotechnical J.* **19** 421–32

Hansen J *et al* 2005 Earth's energy imbalance: confirmation and implications *Science* **308** 1431–5

Hansen J, Ruedy R, Sato M and Lo K 2010 Global surface temperature change *Rev. Geophys.* **48** 4

Hansen J, Sato M, Kharecha P and Schuckmann K v 2011 Earth's energy imbalance and implications *Atmos. Chem. Phys.* **11** 13421–49

Huang S 2006 Annual heat budget of the continental landmasses *Geophys. Res. Lett.* **33** 1851–2004

Kane D L, Hinkel K M, Goering D J, Hinzman L D and Outcalt S I 2001 Non-conductive heat transfer associated with frozen soils *Glob. Planet. Change* **29** 275–92 Inference of Climate Change from Geothermal Data

Knorr W, Prentice I C, House J I and Holland E A 2005 Long-term sensitivity of soil carbon turnover to warming *Nature* **433** 298–301

Koven C D, Riley W J and Stern A 2013 Analysis of permafrost thermal dynamics and response to climate change in the cmip5 Earth system models *J. Clim.* **26** 1877–900

Lawrence D M, Slater A G, Romanovsky V E and Nicolsky D J 2008 Sensitivity of a model projection of near-surface permafrost degradation to soil column depth and representation of soil organic matter *J. Geophys. Res.: Earth Surf.* **113** F02011

Levitus S, Antonov J I, Wang J, Delworth T L, Dixon K W and Broccoli A J 2001 Anthropogenic warming of Earth's climate system *Science* **292** 267–70

Lin X, Smerdon J E, England A W and Pollack H N 2003 A model study of the effects of climatic precipitation changes on ground temperatures *J. Geophys. Res.: Atmos.* **108** 4230

Lyman J M, Good S A, Gouretski V V, Ishii M, Johnson G C, Palmer M D, Smith D M and Willis J K 2010 Robust warming of the global upper ocean *Nature* **465** 334–7

Mann M E, Rutherford S, Bradley R S, Hughes M K and Keimig F T 2003 Optimal surface temperature reconstructions using terrestrial borehole data *J. Geophys. Res.: Atmos.* **108** 4203

Mann M E and Schmidt G A 2003 Ground versus surface air temperature trends: implications for borehole surface temperature reconstructions *Geophys. Res. Lett.* **30** 1607

Mareschal J-C and Beltrami H 1992 Evidence for recent warming from perturbed geothermal gradients: examples from Eastern Canada *Clim. Dyn.* **6** 135–43

Mieville A, Granier C, Liousse C, Guillaume B, Mouillot F, Lamarque J F, Grégoire J M and Pétron G 2010 Emissions of gases and particles from biomass burning during the 20th century using satellite data and an historical reconstruction *Atmos. Environ.* **44** 1469–77

Oleson K W *et al* 2010 Technical description of version 4.0 of the Community Land Model (CLM) *NCAR Technical* NCAR/TN-478+STR (doi:10.1029/2003GL019144)

Pollack H N and Huang S 2000 Climate reconstruction from subsurface temperatures *Annu. Rev. Earth Planet. Sci.* **28** 339–65

Pollack H N and Smerdon J E 2004 Borehole climate reconstructions: spatial structure and hemispheric averages *J. Geophys. Res.: Atmos.* **109** D11106

Roeckner E *et al* 2003 The atmospheric general circulation model ECHAM 5. PART I: Model description *Report/MPI für Meteorologie* 349

Rosenzweig C and Abramopoulos F 1997 Land-surface model development for the giss gcm *J. Clim.* **10** 2040–54

Schmidt G A *et al* 2011 Climate forcing reconstructions for use in pmip simulations of the last millennium (v1.0) *Geosci. Model Dev.* **4** 33–45

Schmidt G A *et al* 2012 Climate forcing reconstructions for use in pmip simulations of the last millennium (v1.1) *Geosci. Model Dev.* **5** 185–91

Schmidt G A and Mann M E 2004 Reply to comment on ground versus surface air temperature trends: implications for borehole surface temperature reconstructions by D chapman *et al Geophys. Res. Lett.* **31** L07206

Smerdon J E, Pollack H N, Cermak V, Enz J W, Kresl M, Safanda J and Wehmiller J F 2004 Air–ground temperature coupling and subsurface propagation of annual temperature signals *J. Geophys. Res.: Atmos.* **109** D21107

Smerdon J E, Pollack H N, Cermak V, Enz J W, Kresl M, Safanda J and Wehmiller J F 2006 Daily, seasonal, and annual relationships between air and subsurface temperatures *J. Geophys. Res.: Atmos.* **111** D07101

Smerdon J E, Pollack H N, Enz J W and Lewis M J 2003 Conduction-dominated heat transport of the annual temperature signal in soil *J. Geophys. Res.: Solid Earth* **108** 2431

Smerdon J E and Stieglitz M 2006 Simulating heat transport of harmonic temperature signals in the Earth's shallow subsurface: lower-boundary sensitivities *Geophys. Res. Lett.* **33** D07101

Sokratov S A and Barry R G 2002 Intraseasonal variation in the thermoinsulation effect of snow cover on soil temperatures and energy balance *J. Geophys. Res.: Atmos.* **107** ACL 13-1–ACL 13-6

Stieglitz M, Déry S J, Romanovsky V E and Osterkamp T E 2003 The role of snow cover in the warming of arctic permafrost *Geophys. Res. Lett.* **30** 1721

Sueyoshi T *et al* 2013 Set-up of the pmip3 paleoclimate experiments conducted using an Earth system model, miroc-esm *Geosci. Model Dev.* **6** 819–36

Taylor K E, Stouffer R J and Meehl G A 2012 An overview of cmip5 and the experiment design *Bull. Am. Meteorol. Soc.* **93** 485–98

von Schuckmann K *et al* 2016 An imperative to monitor Earth's energy imbalance *Nat. Clim. Change* **6** 138–44

Wu T *et al* 2013 An overview of BCC climate system model development and application for climate change studies *J. Meteorol. Res.* **28** 34–56

Yukimoto S *et al* 2012 A new global climate model of the meteorological research institute: Mri-cgcm3 model description and basic performance *J. Meteorl. Soc. Japan* **90** 23–64

Zwally H J, Jun L, Brenner A C, Beckley M, Cornejo H G, Dimarzio J, Giovinetto M B, Neumann T A, Robbins J and Saba J L 2011 Greenland ice sheet mass balance: distribution of increased mass loss with climate warming; 2003–07 versus 1992–2002 *J. Glaciol.* **57** 88–102